

## Diffusion of hydrogen in nickel-based alloys

This article has been downloaded from IOPscience. Please scroll down to see the full text article.

1989 J. Phys.: Condens. Matter 1 2031

(<http://iopscience.iop.org/0953-8984/1/11/011>)

View [the table of contents for this issue](#), or go to the [journal homepage](#) for more

Download details:

IP Address: 171.66.16.90

The article was downloaded on 10/05/2010 at 17:59

Please note that [terms and conditions apply](#).

## Diffusion of hydrogen in nickel-based alloys

K Yamakawa<sup>†</sup>, B Hohler and H Kronmüller

Max-Planck-Institut für Metallforschung, Institut für Physik, Heisenbergstrasse 1,  
7000 Stuttgart 80, Federal Republic of Germany

Received 23 May 1988, in final form 29 September 1988

**Abstract.** The recovery process of hydrogen dissolved in excess in Ni-based alloys is studied by means of the hydrogen quenching method and electrical resistance measurement during isochronal and isothermal annealing treatment. A recovery stage in the electrical resistance due to hydrogen in the alloys shows the same characteristics as observed in the resistance decay of pure Ni in that there is a size dependence of the recovery rate and shape of the isothermal recovery curves. The diffusion coefficients of hydrogen are obtained for the alloys in the range 240–360 K using a similar method to that for pure Ni. The values for the high temperatures investigated are nearly the same as those for pure Ni but at low temperatures, especially for the Ni–0.10 at.% Cu and Ni–0.10 at.% Fe alloys, the coefficients are clearly larger than those for pure Ni. The diffusivity of hydrogen must be depressed by trapping at alloying elements in alloys. This anomalous behaviour suggests that another process—grain boundary diffusion—other than lattice diffusion becomes more important in the low-temperature range.

### 1. Introduction

In recent years, there has been growing interest in the diffusivity of hydrogen in metals and alloys and a large number of measurements of the diffusivity have been made [1]. Among these investigations, hydrogen trapping by solute impurity atoms is observed and causes a reduction in the diffusivity. In contrast with BCC alloys, for FCC alloys there are only a few results available especially for Ni-based alloys. For the magnetic after-effect and internal friction measurement, one jump to the nearest-neighbour site is considered as the elementary process of long-range diffusion. The magnetic relaxation due to the reorientation of diatomic M–H (M ≡ metal) complexes has been investigated for Ni-based alloys containing for example, Fe and Cu [2–4]. From the results the diffusion coefficients of hydrogen are determined for pure Ni by extrapolation with respect to the solute size. Nevertheless the parameters of reorientation of the M–H complex have been obtained from these studies; the parameters may not always correspond to the long-range diffusion of hydrogen in Ni-based alloys.

In pure Ni the recovery process of hydrogen dissolved in excess is studied by measurement of the electrical resistance. The escape of hydrogen from the specimen is formulated by a model calculation and the diffusion coefficient is obtained with high accuracy [5, 6]. For a precise analysis of the recovery of the electrical resistivity due to solute hydrogen the resistivity of the alloy specimen in the hydrogen-free state is required to be as low as

<sup>†</sup> Present address: Applied Physics and Chemistry, Faculty of Engineering, Hiroshima University, Saijoh, Higashi-Hiroshima 724, Japan.

**Table 1.** Chemical composition of Ni-based alloys by atomic absorption spectroscopy.

Alloy	Atomic percentage
Ni-0.1 at.% Cu	$0.102 \pm 0.002$
Ni-0.1 at.% Fe	$0.106 \pm 0.002$
Ni-1.0 at.% Fe	$1.038 \pm 0.002$
Ni-0.05 at.% Ti	$0.049 \pm 0.002$

possible, because both the hydrogen solubility and the resistivity per unit concentration of hydrogen are not too high.

The resistivity increase due to alloying has been reported in [7, 8]. This is about  $4 \text{ n}\Omega \text{ m at.}\%^{-1}$ ,  $8 \text{ n}\Omega \text{ m at.}\%^{-1}$  and  $30 \text{ n}\Omega \text{ m at.}\%^{-1}$  for Ni-Fe, Ni-Cu and Ni-Ti dilute alloys, respectively. Therefore, Fe, Cu and Ti are chosen as the solute elements in Ni-based alloys. The solubilities in Ni of the elements Fe, Cu and Ti are sufficiently high in these alloys.

In the present paper, experiments on the diffusion of hydrogen in Ni-based alloys were carried out using the hydrogen quenching technique similar to that used for pure Ni [5, 6]. The resistivity decay curves are analysed by the same method as for pure Ni and the diffusion coefficients are obtained for the alloys. The diffusion coefficients for the alloys with 0.10 at.% impurities are larger than those for pure Ni, especially at the low temperatures investigated. This enhancement of diffusivity at low temperatures is discussed with relation to grain boundary diffusion.

## 2. Experimental procedure

The electrical resistivity change (decay) due to diffusion of hydrogen out of the cylindrical samples of the Ni-based alloys, in which hydrogen atoms were introduced in excess, are measured at 4.2 K during annealing using a similar method to previous investigations [5, 6].

The alloys Ni-0.10 at.% Cu, Ni-0.10 at.% Fe, Ni-1.0 at.% Fe and Ni-0.05 at.% Ti are produced by melting in an induction furnace and vacuum casting the melt into Mo crucibles. The raw materials used are Ni, Cu, Fe and Ti in the nominal purities 99.998%, 99.999%, 99.998% and 99.97%, respectively; the Ni and Cu were supplied by Koch-Light Laboratories Co. Ltd, the Fe by Johnson Matthey Co. Ltd, and the Ti by Material Research Co. The chemical compositions of prepared alloys are analysed by atomic absorption spectroscopy and the results are given in table 1.

The pre-anneals of the alloy specimens and pure Ni were carried out at 750–770 K in a hydrogen gas atmosphere. The radius of the wire specimens is between 0.050 and 0.100 mm. The experimental apparatus and the method in the present experiment are similar to those used previously for the hydrogen quenching and diffusion experiment on pure Ni [5, 6]. The specimen in the specimen chamber is heated and quenched for hydrogenation in liquid hydrogen or a cooled hydrogen atmosphere. The quenching temperatures are between 1000 and 1200 K.

The electrical resistance of the specimen is measured in liquid He by the standard four-probe method with application of a longitudinal magnetic field of 500 Oe. Use of a magnetic field is necessary to fix the electrical resistance of the magnetic domain wall and to obtain reproducible results during the measurement. The isothermal resistance decays are investigated between 240 and 360 K and isochronal anneals are carried out in a He gas atmosphere up to 420 K.

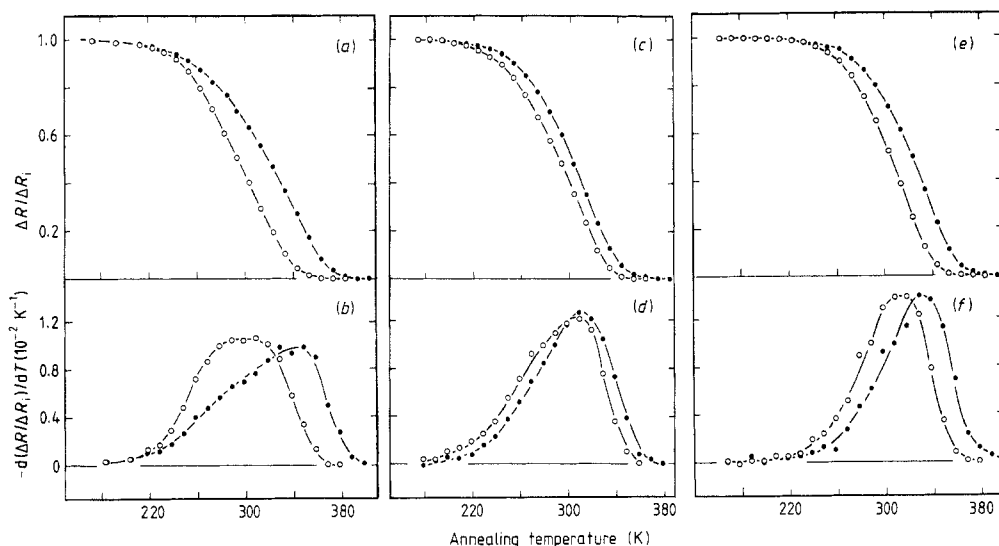


**Figure 1.** Isochronal resistance decay curves and their temperature derivatives of hydrogen-quenched Ni-based alloys for two specimen radii,  $a = 0.050$  mm (open circles) and  $0.078$  mm (full circles). The heating rate is  $10$  K/ $10$  min. (a, b) Ni- $0.10$  at. % Cu, (c, d) Ni- $0.10$  at. % Fe and (e, f) Ni- $1.0$  at. % Fe. On all alloys the recovery rates of  $0.050$  mm specimens are faster than those for  $0.078$  mm specimens.

### 3. Experimental results

#### 3.1. Isochronal annealing

The isochronal resistance decay curves for Ni- $0.10$  at. % Cu, Ni- $0.10$  at. % Fe and Ni- $1.0$  at. % Fe of  $\Delta R/\Delta R_i$ , where  $\Delta R_i$  and  $\Delta R$  are the change in the experimental total resistance and the residual resistance due to solute hydrogen, respectively, are shown for specimens of different sizes in figures 1(a), 1(c) and 1(e). In figures 1(b), 1(d) and 1(f) the temperature derivatives  $-d(\Delta R/\Delta R_i)/dT$  are shown. In the hydrogen-quenched alloy specimens the resistivity decreases in a remarkably similar way to that for pure Ni. One extra smaller peak, which appears at around  $180$  K in pure Ni, is not observed in these alloys. In these figures the decay curves for specimens with the larger radius ( $a = 0.078$  mm) shift to higher temperatures compared with those for the specimens with smaller radius ( $a = 0.050$  mm). The shape of the peak is similar to that of pure Ni. The peak shape of the alloys is a little broader.

#### 3.2. Isothermal annealing

The hydrogen stage is investigated by isothermal annealing in which the specimen is brought to the desired annealing temperature after hydrogen quenching.

The isothermal resistance decay curves for hydrogen-quenched Ni- $0.10$  at. % Cu are shown in figure 2 for specimens with four different radii at the same temperature  $312.2$  K. Although the annealing treatments are the same, the decay rates of the resistance differ considerably corresponding to the results of the size dependence of the above isochronal decay curves. The decay rates for hydrogen-quenched specimens with different radii decrease with increasing specimen size similar to those for pure Ni.

Isothermal decay curves for hydrogen-quenched Ni- $0.10$  at. % Cu, Ni- $0.10$  at. % Fe,

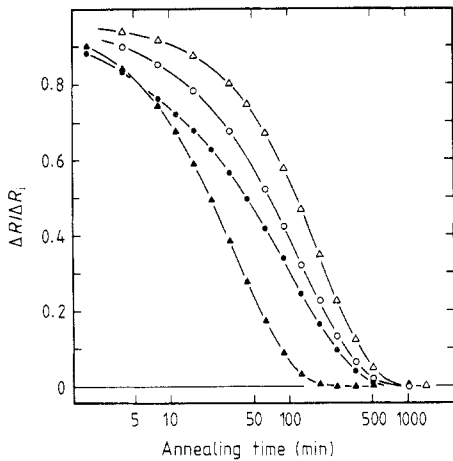


**Figure 2.** Isothermal resistance decay curves for various specimen radii ( $\Delta$ ,  $a = 0.100$ ;  $\circ$ ,  $a = 0.090$ ;  $\bullet$ ,  $a = 0.078$ ;  $\blacktriangle$ ,  $a = 0.050$  mm) of Ni-0.10 at.% Cu wires at the same temperature (312.2 K). The smaller the size becomes, the faster the recovery rate is.

Ni-1.0 at.% Fe and Ni-0.05 at.% Ti alloy are shown in figure 3 for various annealing temperatures. The isothermal decay rate increases with increasing annealing temperature as shown in the figure. The specimen radius  $a$  is 0.050 mm for each alloy except those especially noted. The decay curves are replotted on a linear time scale for the analysis to determine the diffusion constant. For example, figure 4 shows the curves corresponding to figure 3(a). The curves are bent downwards, which suggests that the process does not obey the simple exponential decay similar to the case of pure Ni. It should be noted here that the curves are normalised by  $\Delta R_i$ , which is the experimental total resistance change due to quenched-in hydrogen.

#### 4. Analysis and discussion

The recovery stage which appears in the hydrogen-quenched Ni-based alloys must arise from hydrogen diffusion, because these alloys show similar behaviour to hydrogen-quenched pure Ni [5, 6]. A size dependence of the recovery rate of the isochronal and isothermal decay curves also appears for these alloys; that is, the smaller the specimen radius is, the faster the decay rate becomes. Therefore the main sinks of hydrogen atoms are the external surface of the specimen, as for pure Ni. The stage is analysed by the method reported already for hydrogen diffusion in pure Ni. The hydrogen atoms are quenched in the specimens with a uniform distribution using the ideal quenching technique (infinite quenching rate) and as a result of the annealing treatment the hydrogen atoms diffuse to the specimen surface and leave the specimen, forming a concentration gradient in the specimen following the diffusion equation. The finite quenching rate in the experiment is taken into account as part of the annealing process. The diffusion coefficient is obtained from a comparison between the experimental isothermal decay curves and the calculated isotherms. A precise description of the calculation and analysis has already been given in previous papers [5, 6].

A characteristic of these curves for the alloy specimens is that the base resistance ratio  $R_B/\Delta R_0$  (where  $R_B$  and  $\Delta R_0$  are the residual resistance of the specimen from which hydrogen is fully annealed out and the ideal total resistance change for infinite quenching rate, respectively) is larger than those for pure Ni. Usually the values of  $R_B/\Delta R_0$  are

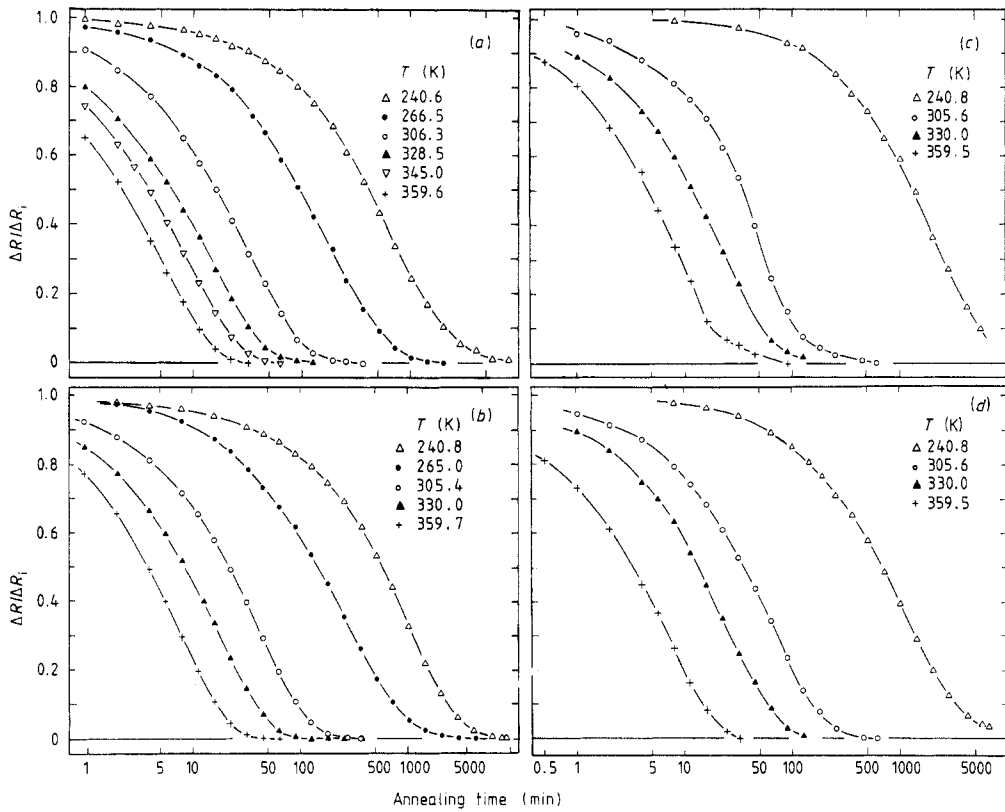


**Figure 3.** Isothermal resistance decay curves at several temperatures for Ni-based alloys. The specimen radius is  $a = 0.050$  mm. (a) Ni-0.10 at.% Cu, (b) Ni-0.10 at.% Fe, (c) Ni-1.0 at.% Fe and (d) Ni-0.05 at.% Ti.

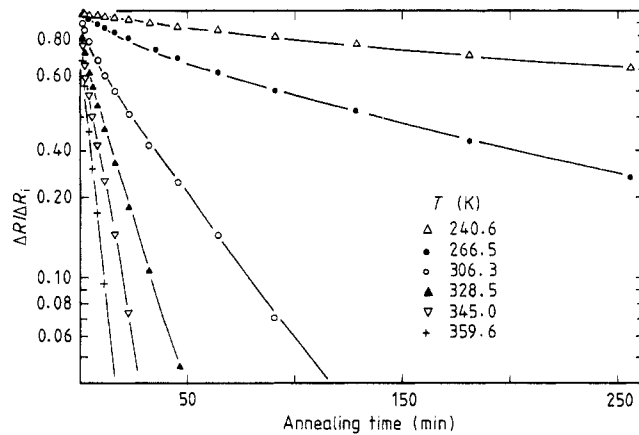


**Figure 4.** Isothermal decay curves at several temperatures for Ni-0.10 at.% Cu replotted with linear timescale from figure 2. The curves are calculated from the method described for pure Ni [5, 6].

0.3–1, 3–6, 1–2, 5–7 and 12–16 for pure Ni, Ni–0.10 at.% Cu, Ni–0.10 at.% Fe, Ni–1.0 at.% Fe and Ni–0.05 at.% Ti, respectively. As shown in figure 9 of the previous paper [5], the calculated isothermal decay curves for large  $R_B/\Delta R_0$  are bent downwards less. In fact, all decay curves show the tendency compared with those of pure Ni. Some of the isotherms are shown in figure 4 for Ni–0.10 at.% Cu specimens. The full curves are the results of the calculation [5]. The agreement between the experiment and calculation is also very good for other alloys except for Ni–Ti alloy. From these data fits the diffusion coefficients are obtained for various annealing temperatures, in a similar way to those for pure Ni. As the increase in residual resistivity due to impurity atom addition is large in Ni–0.05 at.% Ti as mentioned before, the hydrogen resistance  $\Delta R_i$  or  $\Delta R_0$  relative to the residual resistance  $R_B$  becomes smaller than for other Ni-based alloys. Therefore the accuracy of the hydrogen resistance measurement becomes worse.

The surface barriers have no effect on hydrogen diffusion, at least in the Ni-based alloys used in the present study, because the diffusion coefficients have similar values for the specimens with different radii. For pure Ni, it is demonstrated that there is no surface barrier because the generalised calculated curve and the resistivity data agree with each other with respect to annealing temperature and specimen size, as shown in figure 7 of the previous paper [6].

The diffusion coefficients of hydrogen are shown in figure 5 plotted against the reciprocal temperature  $1/T$ , together with the results for pure Ni [6]. The diffusion coefficients for the alloys at high temperatures in the investigated temperature range are nearly the same as those for pure Ni, as shown in the figure. The values for Ni–0.10 at.% Cu and Ni–0.10 at.% Fe at low temperatures, however, are clearly larger than that of pure Ni. The values for Ni–1.0 at.% Fe are nearer to the values for pure Ni than those for Ni–0.10 at.% Cu and Ni–0.10 at.% Fe. For Ni–0.05 at.% Ti the diffusion coefficients show a large scatter because of the smaller ratio of the hydrogen resistance to the total specimen resistance mentioned above. This enhancement of diffusivity due to alloying at a low temperature is a very strange behaviour for hydrogen diffusion in a solid if the mechanism is based on the trapping model in which the hydrogen atoms are trapped at alloying impurity atoms. In the model the hydrogen diffusion coefficient must become smaller than that of the pure material [9, 10]. In [9], a report is given of investigations of hydrogen–impurity complexes in various Ni-based alloys and the binding enthalpies, which range from 7.72 to 11.7 kJ mol<sup>-1</sup> for Ni–Fe, Ni–Cu and Ni–Ti alloys, of hydrogen–impurity complexes were obtained. These binding enthalpies affect the hydrogen diffusivity in the present Ni-based alloys especially in the lower-temperature range. In [9] the diffusion coefficient  $D_A$  of the alloy was obtained from the hydrogen-trapping model at impurity atoms in dilute alloys over a limited temperature range:

$$D_A = D_{0A} \exp(-E_A/RT) \quad (1)$$

$$E_A = E + (C_{M-H}/C_H)E_B \quad (2)$$

$$\ln D_{0A} = \ln D_0 + \ln[(1 - C_{M-H}/C_H)/(1 - 6C_M)] + (C_{M-H}/C_H)(E_B/RT) \quad (3)$$

$$C_{M-H} = C_H[6C_M/(1 - 6C_M)] \exp(-S_B/R) \exp(E_B/RT)/1 + (6C_M/(1 - 6C_M)) \times \exp(-S_B/R) \exp(E_B/RT) \quad (4)$$

where  $E$ ,  $D_0$  and  $C_H$  are the activation energy, the pre-exponential factor of diffusion and the hydrogen concentration in the specimen, respectively, for pure Ni and  $C_M$ ,  $C_{M-H}$ ,  $E_B$  and  $S_B$  are the substitutional impurity concentration, the metallic impurity–hydrogen complex concentration in equilibrium, the binding energy of the complex and

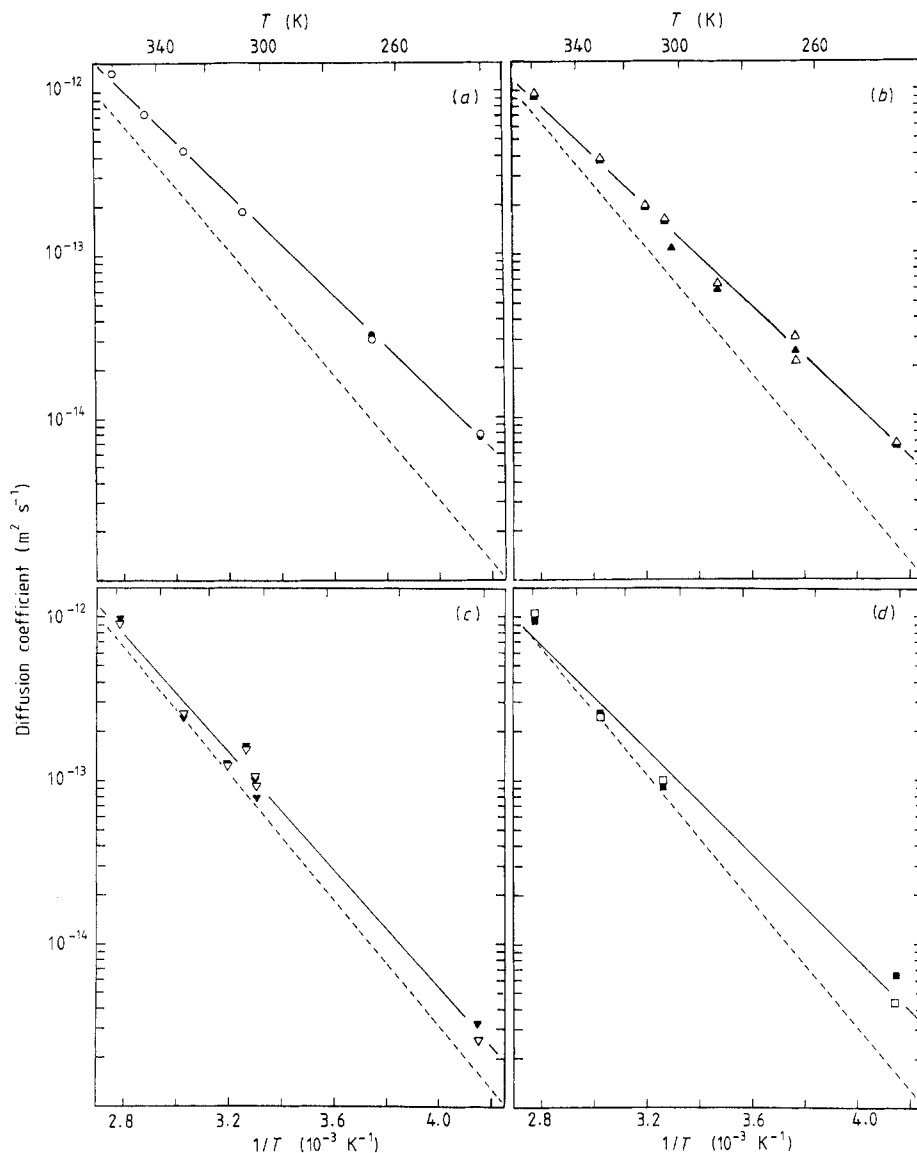


**Figure 5.** The obtained diffusion coefficient of hydrogen plotted against reciprocal temperature for Ni-based alloys with that for pure Ni. The broken line shows the coefficient for pure Ni. All specimens are of radius 0.050 mm. The diffusion coefficients for the alloys are clearly larger than for pure Ni at low temperatures. (a) Ni-0.10 at.% Cu, (b) Ni-0.10 at.% Fe, (c) Ni-1.0 at.% Fe and (d) Ni-0.05 at.% Ti. Each pair of symbols (open and full) corresponds to values obtained for different specimens at the same time.

the binding entropy of the complex, respectively [9]. The values of  $D_A$  are calculated with  $S_B = 0$  for Ni-0.10 at.% Cu, Ni-0.10 at.% Fe, Ni-1.0 at.% Fe and Ni-0.05 at.% Ti, respectively, and are shown in figure 6 with the line  $D = 1.90 \times 10^{-7} \times \exp(37.19 \text{ kJ mol}^{-1}/RT) \text{ m}^2 \text{ s}^{-1}$  for pure Ni. The parameters used are tabulated in table 2. In the trapping model the diffusion coefficient for the alloys must become considerably smaller than that for pure Ni.



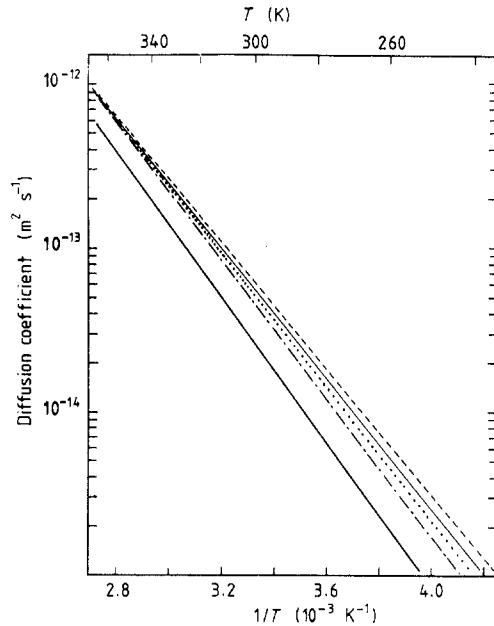


**Figure 6.** Diffusion coefficients of hydrogen calculated from equations (1)–(4) with  $S_B = 0$  by the hydrogen-trapping model. -----, Ni–H; ····, Ni–0.10 at.% Cu–H; —, Ni–0.10 at.% Fe–H; - - - - - , Ni–1.0 at.% Fe–H; — · — · — , Ni–0.05 at.% Ti–H.

**Table 2.** The parameters for the calculation of diffusion coefficient in figure 6. The values of  $E_B$  are taken from [9].

Alloy	$C_M$ (at.%)	$E_B$ (kJ mol <sup>-1</sup> )
Ni–0.1 at.% Cu	0.1	9.17
Ni–0.1 at.% Fe	0.1	7.72
Ni–1.0 at.% Fe	1.0	11.7
Ni–0.05 at.% Ti	0.05	

**Table 3.** Diffusivity constants of hydrogen.

Alloy	$D_0$ (10 <sup>-8</sup> m <sup>2</sup> s <sup>-1</sup> )	$E$ (kJ mol <sup>-1</sup> )	Temperature range (K)
Ni–0.1 at.% Cu	3.19 ± 0.38	30.56 ± 0.28	240–360
Ni–0.1 at.% Fe	1.57 ± 0.31	29.34 ± 0.47	240–360
Ni–1.0 at.% Fe	8.04 ± 2.60	34.27 ± 0.79	240–360
Ni–0.05 at.% Ti	2.06 ± 0.89	30.60 ± 1.05	240–360
Ni <sup>a</sup>	19.0 ± 1.1	37.19 ± 0.13	220–330

<sup>a</sup> [6].

From the above-mentioned argument the diffusion of hydrogen atoms in the alloys is not caused by one process but by two processes, i.e. lattice diffusion and boundary diffusion. Nevertheless, straight lines are obtained in Arrhenius plots for various Ni-based alloys in the temperature range investigated. The activation energy  $E_A$  and the pre-exponential factor  $D_{0A}$  are evaluated from figure 5 using the method of least squares for the temperature range between 240 and 360 K and are given with the values for pure Ni in table 3. Owing to the anomalous high diffusivity at low temperatures the activation

energies and pre-exponential factors become smaller for the alloys than for pure Ni.

A report of an investigation on the hydrogen diffusion in pure Ni with various grain sizes is given in [11] and it was concluded that grain boundary diffusion of hydrogen did not take place in the temperature range (300–770 K) investigated. Recently [12], the grain boundary diffusion of hydrogen in pure Ni was detected. It was reported that the diffusion coefficient of hydrogen for boundary diffusion was approximately 60 times larger than for lattice diffusion and that boundary diffusion was about one thousandth of the lattice diffusion at 25 °C [13] for the grain boundary content in their specimen. This extremely small contribution from the boundary diffusion of hydrogen is responsible for the fact that no boundary diffusion above room temperature was detected in [11]. Because the activation energy in the boundary diffusion of hydrogen is smaller than in lattice diffusion, boundary diffusion becomes important at low temperatures. For Ni–1.0 at.% Fe a decrease in hydrogen diffusion through the lattice and boundary due to trapping at the alloying element may be cancelled on increase in the boundary diffusion ratio. This means that the ratio of boundary diffusion increases from pure Ni to Ni–0.10 at.% Cu and Ni–0.10 at.% Fe but that the ratio increases less from Ni–0.10 at.% Fe to Ni–1.0 at.% Fe.

The grain size of pure Ni and the alloys are observed by optical microscopy after pre-annealing at 1000 °C for 5 h. The size varies widely in different parts of the specimen, especially for pure Ni. The mean sizes are about 135  $\mu\text{m}$ , 65  $\mu\text{m}$ , 70  $\mu\text{m}$ , 50  $\mu\text{m}$  and 50  $\mu\text{m}$  for pure Ni, Ni–0.10 at.% Cu, Ni–0.10 at.% Fe, Ni–1.0 at.% Fe and Ni–0.05 at.% Ti, respectively. For pure Ni the mean size is larger than the specimen diameter. The grain boundary diffusion in pure Ni is negligibly small compared with the lattice diffusion. For the alloys the mean size is one half to one third of that for pure Ni. Boundary diffusion may affect the hydrogen diffusion constant considerably because of this size change. For example, if we assume that the boundaries are perfect sinks for hydrogen atoms, the roughly estimated apparent diffusion constant is  $2^3$ – $3^3$  times larger than that for pure Ni. Because the boundaries are not perfect sinks in practice, the apparent increase in hydrogen diffusivity in the alloys is below the same order of magnitude of lattice diffusion in pure Ni at around room temperature.

In order to clarify the grain boundary diffusion of hydrogen, it would be interesting to carry out the diffusion experiment for single crystals and polycrystals at low temperatures.

### Acknowledgments

The authors would like to express their appreciation to H Maisch and R Henes for their technical assistance and to the other technical staff of the Max-Planck-Institut for continuous support during this experiment.

One of the authors (KY) wishes to acknowledge Professor A Seeger (Max-Planck-Institut), Professor H Schultz (Max-Planck-Institut) and Professor F E Fujita (Osaka University) for continuous encouragement throughout this study. The financial support to a visiting scientist by the Max-Planck Institut is gratefully acknowledged by KY.

### References

- [1] Völkl J and Alefeld G 1978 *Hydrogen in Metals* vol I, ed. G Alefeld and J Völkl (Berlin: Springer) p 321
- [2] Hohler B and Kronmüller H 1982 *Phil. Mag.* **45** 607

- [3] Hohler B and Kronmüller H 1981 *Phil. Mag.* **43** 1189
- [4] Hohler B and Schreyer H 1982 *J. Phys. F: Met. Phys.* **12** 857
- [5] Yamakawa K, Tada M and Fujita F E 1976 *Japan. J. Appl. Phys.* **15** 769
- [6] Yamakawa K and Fujita F E 1977 *Japan. J. Appl. Phys.* **16** 1747
- [7] Farrell T and Greig D 1968 *J. Phys. C: Solid State Phys.* **1** 1359
- [8] Fert A and Cambell I A 1976 *J. Phys. F: Met. Phys.* **6** 849
- [9] Hohler B and Kronmüller H 1979 *Z. Phys. Chem., NF* **114** 93
- [10] Oriani R A 1970 *Acta Metall.* **18** 147
- [11] Robertson W M 1973 *Z. Metallk.* **64** 436
- [12] Tsuru T and Latanision R M 1982 *Scr. Metall.* **16** 575
- [13] Latanision R M 1988 private communication